

Magnetoluminescence of highly excited InAs/GaAs self-assembled quantum dots

P. P. Paskov,^{1,*} P. O. Holtz,¹ B. Monemar,¹ J. M. Garcia,² W. V. Schoenfeld,² and P. M. Petroff²

¹*Department of Physics and Measurement Technology, Linköping University, S-581 83 Linköping, Sweden*

²*Materials Department, University of California, Santa Barbara, California 93106*

(Received 19 January 2000)

We present magnetoluminescence measurements of InAs/GaAs self-assembled quantum dots (QD's) at different excitation intensities. By applying high excitation intensities, the magnetic field evolution of the excited-state emission of QD's is revealed. A splitting of the states with a nonzero magnetic momentum is observed and the in-plane reduced electron-hole mass is determined. The experimental value is found to be in a good agreement with the theoretical predictions based on the eight-band $\mathbf{k}\cdot\mathbf{p}$ model including both strain effect and band nonparabolicity. The density dependence of the diamagnetic shift of the ground-state emission is also studied providing evidence for screening of the Coulomb interaction in QD's.

I. INTRODUCTION

In recent years, a lot of attention has been devoted to the study of the quantum-dot (QD) semiconductor heterostructures. The strong interest in these systems is motivated, not only by their potential for applications in optoelectronic devices but also by their fundamental physical properties occurring when the carriers are spatially confined by a three-dimensional potential.¹ The spatial confinement of both electrons and holes in the dot region implies an increase of the Coulomb interaction strength and a formation of excitons. Therefore, the electronic structure and the resultant optical transitions of the dots are determined by the interplay of the quantum confinement and the electron-hole correlation.² Among the various fabrication techniques, the self-assembled growth, based on the Stranski-Krastanow mechanisms, is considered to be the most promising one because it results in high-quality dislocation-free QD's.³ In particular, the InAs QD's grown by this method on lattice-mismatched GaAs substrate reveal a strong luminescence at 1.1–1.3 eV, exhibiting a well-defined zero-dimensional character of the density of states.^{4,5} The self-assembled growth typically provides QD's with dimensions comparable to the exciton Bohr radius. In this strong confinement regime, the size quantization is expected to overcome Coulomb effects. However, the extent to which the presence of excitons affects the energy spectrum is still a crucial point in the understanding the optical spectra, especially in highly excited QD's.⁶

Valuable information about the excitons and the carriers confined in the QD's can be obtained from optical spectra perturbed by an external field such as a magnetic field. The magnetic field introduces strong but predictable modification of the electronic structure. In the case of a low field applied, the wave functions exhibit only a small perturbation resulting in a diamagnetic shift of the states. At the high-field limit, where the cyclotron energy is larger than both the lateral confinement energy and the exciton binding energy, the magnetic confinement dominates and a Landau-level-like structure is expected to occur. Moreover, the magnetic field removes the degeneracy of the states and gives rise to qualitatively different magnetic field dependence of the ground- and excited-state emission. The diamagnetic shift and the spin splitting in QD's have been measured in low-excitation intensity experiments by a number of authors.^{7–13} However,

only a limited number of works on the magneto-optical properties of the highly excited QD's have been reported up to date. The magnetoluminescence spectra in shallow etched,¹⁴ strain-induced,¹⁵ and self-assembled¹⁶ In_xGa_{1-x}As/GaAs QD's have exhibited a splitting of the excited-state emission. The spectra have been interpreted in terms of single particles^{14,15} or of a gas of weakly interacting excitons.¹⁶ The photoluminescence (PL) and photoluminescence excitation (PLE) measurements in a magnetic field have also been performed for InAs/GaAs QD's with the purpose to study the effect of many-body Coulomb interactions.¹⁷ Up to now, the Landau-level formations have been observed only in self-assembled InP/In_yGa_{1-y}P QD's.¹⁸

In this paper, we report on magnetoluminescence studies of self-assembled InAs/GaAs QD's at different excitation intensities. The magnetic field dependence of the excited states is investigated and the electron-hole reduced mass is determined. Good agreement is found with the carrier effective mass calculated by applying the eight-band $\mathbf{k}\cdot\mathbf{p}$ model to strongly strained InAs. We have also been able to elucidate the role of the screening of the Coulomb interaction in QD's by studying the intensity dependence of the diamagnetic shift.

II. EXPERIMENT

The QD samples for the present study were grown by molecular beam epitaxy (MBE) in a Varian GEN II system under arsenic pressure of 1×10^{-5} Torr.¹⁹ On top of an n^+ -doped GaAs(100) substrate, a short-period (40×2 nm/2 nm) GaAs/AlAs superlattice was grown at a temperature of $T_g = 630^\circ\text{C}$, followed by the deposition of a 200-nm-thick GaAs buffer layer at $T_g = 580^\circ\text{C}$ with substrate rotation. At a temperature of 530°C , 1.7 monolayers of InAs were deposited, followed by a growth interruption of 30 s to narrow the size distribution. For this thickness of InAs, self-assembled growth was initiated and InAs islands were formed on the surface.³ Then the islands were overgrown with 1-nm-thick GaAs, while the substrate temperature was maintained at 530°C followed by a second 30-s growth interruption. Atomic force microscopy (AFM) after such a growth procedure revealed well-defined islands of lateral dimension $2r \approx 60$ nm, height $h \approx 1.5$ nm, and density $\approx 1 \times 10^{10} \text{ cm}^{-2}$.¹⁹ A final 50-nm-thick GaAs capping layer

was grown at a temperature of 580 °C to further protect the QD's layer.

The magneto-PL measurements were performed at a temperature of $T=2$ K. The sample was mounted in the helium insert of a cryostat with a superconducting magnet providing a field of up to 14 T. The field was applied parallel to the growth direction (z axis) of the sample. The optical excitation from an Ar^+ laser ($\lambda_{\text{ex}}=514.5$ nm) was fed to the sample through a multimode optical fiber with a core diameter of 200 μm . The emitted luminescence signal was collected through the same fiber and then dispersed by a 0.85-m double monochromator and detected by a cooled $\text{In}_x\text{Ga}_{1-x}\text{As}_y\text{P}_{1-y}/\text{InP}$ photomultiplier tube (Hamamatsu R5509-42) using a conventional lock-in technique. The detection system provided a spectral resolution of 0.2 nm.

III. RESULTS

The magneto-PL spectra of the QD's were measured at an excitation intensity ranging from 2.5 to 570 W/cm^2 . At low-excitation conditions only a single peak, originating from the ground-state emission of the QD's, is observed [Fig. 1(a)]. The peak exhibits a full width at half maximum (FWHM) of 25 meV reflecting a relatively high homogeneity in the dot sizes. When a magnetic field is applied, the peak shifts towards higher energies without noticeable change in the shape. At excitation intensities above 40 W/cm^2 a novel higher-energy peak attributed to the emission from the excited state of QD's appears in the zero-field PL spectrum. With further increasing excitation intensity, the ground-state emission saturates and a third peak appears in the spectrum. At the highest excitation intensity used ($I_{\text{exc}}=570$ W/cm^2) the PL spectrum is dominated by the first excited-state emission [Fig. 1(b)]. The emission of the InAs wetting layer (WL) at 1.423 eV is also observed. Applying a magnetic field results in a complicated structure in the high-excitation PL spectra. Besides the blue shift of the ground-state and wetting-layer emissions, there is a splitting of the peaks corresponding to the excited-state emissions. To exactly determine the energy position of the different peaks, a multiple Gaussian fit of each spectrum was performed. Such a deconvolution is found to be quite accurate due to the smooth line shapes of the spectra and allows us to draw the fan plots of the energies as a function of the magnetic field. The fan plots extracted from the magnetoluminescence data in Fig. 1(b) are presented in Fig. 2. It is clearly seen that the peak corresponding to the first excited state exhibits a nearly symmetric splitting into two components, while the peak corresponding to the second excited state splits into three components. The energy difference between the two components of the first excited-state emission increases linearly with the magnetic field and reaches a value of 30 meV at $B=14$ T (see the inset in Fig. 2). Almost the same value is obtained for all excitation intensities for which the excited-state emission is observed.

IV. DISCUSSION

A. Electronic states and optical transitions in a magnetic field

To analyze the magnetoluminescence data we have to consider the magnetic interaction affecting a particle in a

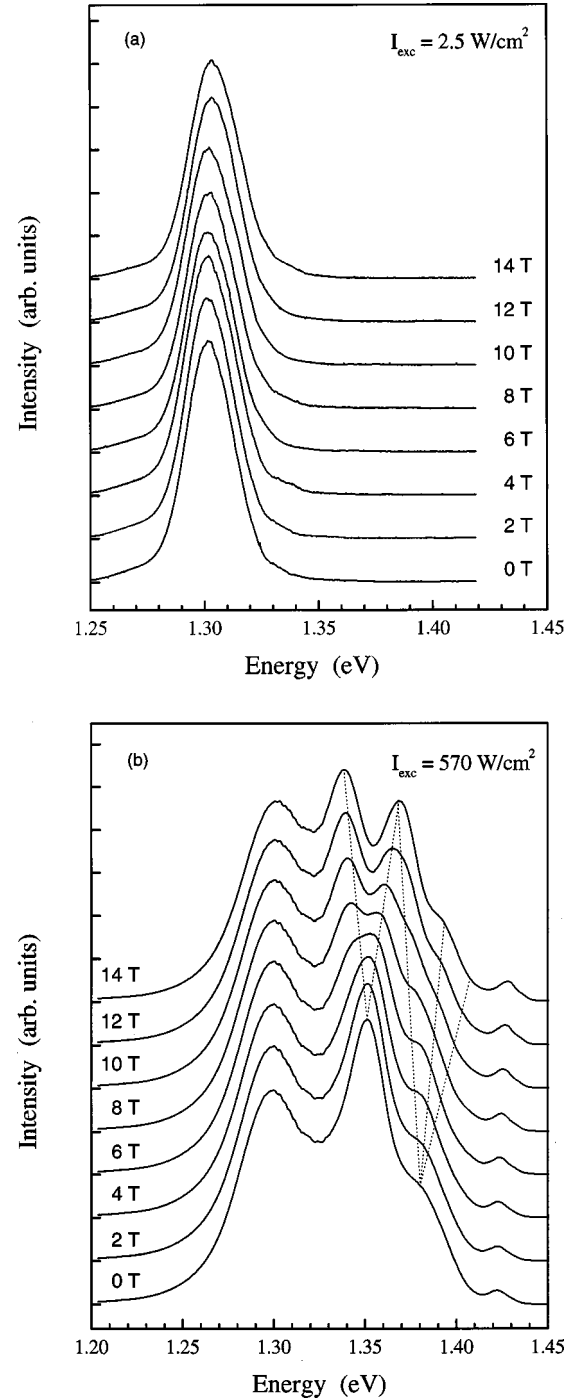


FIG. 1. Photoluminescence spectra of QD's at different magnetic fields and an excitation intensity of (a) $I_{\text{exc}}=2.5$ W/cm^2 and (b) $I_{\text{exc}}=570$ W/cm^2 , respectively. The dashed lines connect split transitions arising from single one at $B=0$ T.

potential of cylindrical symmetry. Detailed numerical calculations have shown that in lens-shaped InAs/GaAs QD's both electrons and holes are confined by an effective parabolic potential.²⁰ The bound states are characterized by the quantum number n_r specifying the number of radial modes and by the angular momentum m . At zero magnetic field, the energies of discrete states form the spectrum consisting of degenerate and almost equally spaced shells. The ground states ($n_r=0$, $m=0$) have an s -like character and can be occupied by only two carriers with an opposite spin. The

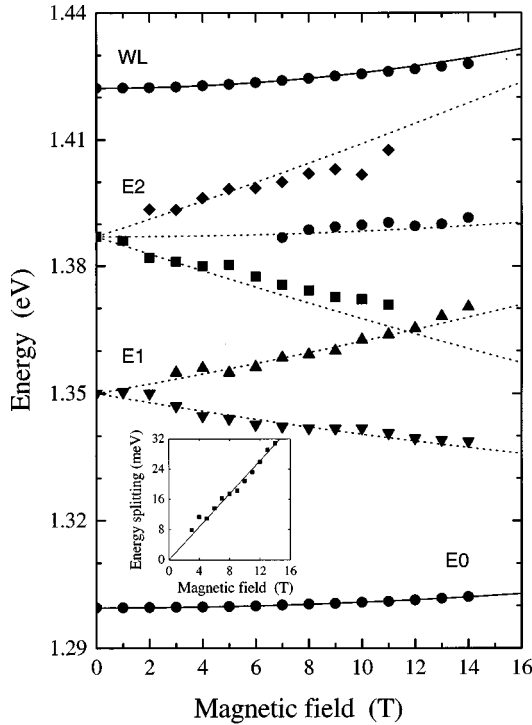


FIG. 2. Magnetic field dependence of the energy position of the QD emission peaks (E0, E1, and E2) and the wetting layer emission (WL) at an excitation intensity of $I_{\text{exc}} = 570 \text{ W/cm}^2$. The solid lines show a fit to the experimental data, while the dashed lines are calculated by the Zeeman term with a reduced mass $\mu = 0.053m_0$ and the measured diamagnetic coefficient ($\gamma_2 = 13.2 \mu\text{eV/T}^2$). The inset shows the field dependence of the splitting of the E1 emission.

next higher p -like ($n_r = 1$, $m = \pm 1$) and d -like ($n_r = 2$, $m = 0, \pm 2$) shells can hold up to four and six carriers, respectively. The parity of the electron and hole wave functions yields a selection rule for the interband transitions $\Delta m = \text{even}$, but the strongest transitions are those between states having the same radial quantum number.²¹ Therefore the zero-field PL spectrum should be dominated by peaks corresponding to the electron-hole recombination between equivalent shells. Nevertheless, the higher-energy peaks in the PL spectra of small pyramidal QD's are often interpreted as transitions between the electron ground state and the hole excited states.^{17,22} This interpretation is based on the theoretical predictions that there is only one confined electron state in this kind of dot. In the lens-shaped QD's studied here, however, the existence of several confined electron states is not only predicted by theory²⁰ but is also confirmed by the capacitance (C - V) measurements.²³ Therefore we identify the three peaks observed in the PL spectra at zero field as arising from s - s , p - p , and d - d transitions, respectively.

The application of a magnetic field parallel to the growth axis results in three apparent effects on the spectrum of the QD's. (1) The angular momentum degeneracy of the excited states is removed and depending on the sign of m , the levels shift linearly towards lower or higher energy with increasing magnetic field (Zeeman effect). The shift is given by $\Delta E_Z = e\hbar Bm/2\mu$, where μ is the in-plane reduced electron-hole mass.¹⁵ (2) All states split into two components due to the lifting of the spin degeneracy. The energy difference between the components is $\Delta E_S^{e,h} = g_{e,h}m_B B$, where $g_{e,h}$ is the

electron (hole) g factor and m_B is the Bohr magneton.¹³ (3) All split states exhibit a diamagnetic shift quadratic with the field, $\Delta E_D = \gamma_2 B^2$, where the diamagnetic coefficient γ_2 depends on both the carrier effective masses and the extent of the wave functions.⁷⁻¹²

This single-particle model describes in a quite satisfactory way the magnetic field evolution of the PL spectra of QD's studied here. The ground-state emission blueshifts proportionally to B^2 (see Sec. IV C), while the excited-state emissions reveal in addition a Zeeman splitting. The spin splitting in $\text{In}_x\text{Ga}_{1-x}\text{As}/\text{GaAs}$ QD's is of the order of 0.1 meV/T (Ref. 13) and cannot be resolved in our unpolarized PL spectra of an ensemble of dots. The dashed lines in Fig. 2 represent the magnetic field dependence of the peak energies obtained as the measured diamagnetic shift is added to the Zeeman term calculated with the reduced mass of $\mu = 0.053m_0$ to be determined below, where m_0 is the free-electron mass.

It is worth noting that the single-particle picture will be modified if the electron-hole correlation effects are taken into account. The presence of excitons results in a diamagnetic shift substantially smaller than that of the single-particle states due to the additional confinement of the exciton wave function in the dots.¹⁵ Moreover, the magnetic correction to the excited states is different for excitons and uncorrelated carriers. Since only the excitons with zero total angular momentum can decay radiatively by an allowed interband transition, the Zeeman splitting cannot be observed.^{10,24,25} Thus the splitting can be a measure of whether the emission has an excitonic or a single-particle nature. The lateral confinement energy in the dot studied here ($E_e + E_h = 45 \text{ meV}$) is comparable to the characteristic Coulomb energy [$\approx 20 \text{ meV}$ (Refs. 16 and 20)], and we can expect that the Coulomb correlation effects to some extent influence the energy spectrum of QD's. Nevertheless, the magnetoluminescence spectra monitored resemble very well the spectra of uncorrelated electron-hole pairs. This fact is attributed to the screening of the Coulomb interaction when several electron-hole pairs are excited in a single dot. The observation of a third component of the emission originating from d - d transitions implies a minimum dot occupancy of 11–12 for at least some of the dots. This corresponds to a three-dimensional (3D) carrier density of about $5 \times 10^{18} \text{ cm}^{-3}$ at which the screening is expected to be significant. The importance of the screening in our magneto-PL measurements is confirmed by the excitation dependence of the diamagnetic shift as will be elucidated below.

B. Effective masses

The observation of the Zeeman splitting allows an in-plane reduced mass to be determined. This was done by a linear fit of the magnetic field dependence of the energy separation $\Delta E_{\pm 1} = e\hbar B/\mu$ between the two components of the first excited-state emission. The values of μ obtained at different excitation intensities are given in Table I. All values are slightly dispersed around $\mu = 0.053m_0$. In a strained InAs layer on GaAs (lattice mismatch $\sim 7\%$), the heavy-hole band is the uppermost valence band, while the light-hole band is shifted downwards in energy by 206 meV .²⁶ Then only heavy-hole states are involved in the interband transi-

TABLE I. Electron-hole reduced mass μ , diamagnetic coefficient γ_2 , and lateral extent of the ground-state wave function $\sqrt{\langle \rho^2 \rangle}$ determined from the magnetoluminescence spectra of QD's at different excitation intensities.

Excitation intensity (W/cm ²)	μ (units of m_0)	γ_2 ($\mu\text{eV}/\text{T}^2$)	$\sqrt{\langle \rho^2 \rangle}$ (nm)
2.5		7.8 ± 0.2	4.35 ± 0.05
50	0.053 ± 0.001	8.7 ± 0.3	4.58 ± 0.07
100	0.0546 ± 0.0006	9.6 ± 0.2	4.81 ± 0.05
250	0.0534 ± 0.004	11.3 ± 0.1	5.23 ± 0.04
356	0.0526 ± 0.0006	12.3 ± 0.2	5.45 ± 0.05
500	0.0529 ± 0.007	13.0 ± 0.2	5.60 ± 0.07
570	0.0531 ± 0.008	13.2 ± 0.1	5.65 ± 0.04

tions in QD's. Accordingly, the obtained mass corresponds to the reduced electron-heavy-hole mass. In comparison with the bulk InAs it is found that the reduced mass in the QD's is enhanced by a factor larger than 2. This can be explained by the strain-induced modification of the carrier effective masses. The strain and the band nonparabolicity considerably enhance the electron effective mass, while the in-plane heavy-hole mass is reduced and shows a "light-hole" character.^{9,17}

To clarify the enhancement of the reduced mass, we separately estimate the carrier effective masses in strained InAs. First, we calculate the strain-modified electron mass assuming an average hydrostatic strain in the dot region. Although the actual strain distribution is more complicated, this approximation seems to be quite reasonable for our flat dots.²⁷ The band-edge electron mass, assumed to be isotropic, is determined by employing the eight-band $\mathbf{k} \cdot \mathbf{p}$ model, where the influence of the remote bands on the conduction and valence states is included.²⁸ The calculation with the deformation potentials and the elastic constants taken from Ref. 29 and Kane's parameter $E_p = 22.2$ eV yields a value of $m_e = 0.050m_0$. Afterwards, the conduction-band nonparabolicity is determined within the same model.²⁸ The electron and hole z -confinement energies $E_{e,z}$ and $E_{h,z}$ are calculated for a rectangular quantum well (QW) potential with strained band offsets $\Delta E_e = 0.540$ eV and $\Delta E_h = 0.400$ eV,^{27,30} the strain-independent effective heavy-hole mass in the z direction $m_{hh,z} = 0.34m_0$, and the effective electron mass value at the band edge. In this treatment, the thickness L_z of the QW is used as a free parameter in order to fit the ground-state emission of QD's at $E_0 = 1.303$ eV with the sum of the z -confinement energy ($E_{e,z} + E_{h,z}$) and the lateral confinement energy ($E_e + E_h = 45$ meV). We note that the band offsets used originate from an unstrained valence-band offset $E_{vbo} = 263$ meV (Refs. 27 and 29) and are consistent with the recent experimental results for an ultrathin InAs layer embedded in GaAs.³⁰ A good fit is obtained for $L_z = 1$ nm and the electron z -confinement energy is found to be 450 meV. The electron effective mass corresponding to such an energy is $m_e = 0.081m_0$. This value is a little bit higher than that estimated by Wilson *et al.*,¹⁷ but is very close to the experimental data from both the resonant tunneling and the infrared absorption measurements.^{31,32}

In the decoupled heavy-hole-light-hole limit, the in-plane heavy-hole mass in a bulk unstrained InAs is $m_{hh} = (\gamma_1^L$

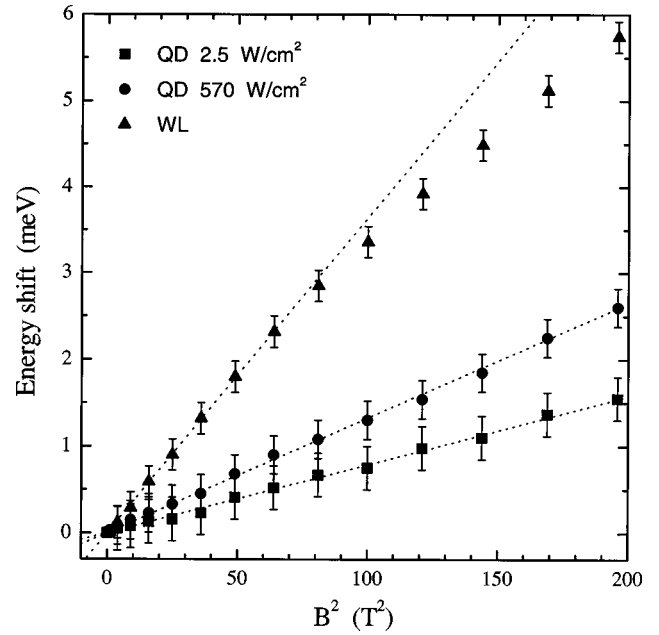


FIG. 3. Energy shift of the QD ground-state emission and the WL emission vs the square of the magnetic field. The dashed lines show a linear fit to the experimental data.

$+ \gamma_2^L)^{-1}m_0 = 0.036m_0$, where γ_1^L and γ_2^L are the usual valence-band Luttinger parameters, but the strain increases this value, similarly to the electron mass. A simple way to estimate the enhancement of the heavy-hole mass is to calculate it with the strain-modified eight-band Luttinger parameters, which results in a value of $m_{hh} = 0.112m_0$. However, such an approach does not include the effects of the valence-band mixing and the nonparabolicity that are expected to be significant due to the large heavy-hole z -confinement energy. Taking this into account, the evaluated value of $m_{hh} = 0.153m_0$ obtained from the experimentally determined reduced mass and the calculated electron mass corresponds to a reasonable value for the in-plane heavy-hole mass.

C. Diamagnetic shifts

The magnetic field dependence of the ground-state energy shift for the QD's at excitation intensities of 2.5 and 570 W/cm² is shown in Fig. 3. The lines represent the least-square fit of the experimental data. The shift is quadratic with the magnetic field in the entire field region investigated. This means that the extent of the ground-state wave function is smaller than the magnetic length $l_c = (\hbar/eB)^{1/2}$ ($l_c = 6.9$ nm at $B = 14$ T) and the high-field region cannot be reached. The values of the diamagnetic coefficient γ_2 extracted from the fit at different excitation intensities are plotted in Fig. 4. It is evident that the γ_2 increases with the intensity and seems to approach a saturation at a high-excitation-intensity level.

The diamagnetic coefficient in the QD's is given by^{7,11,15}

$$\gamma_2 = \frac{e^2}{8\mu} \langle \rho^2 \rangle, \quad (1)$$

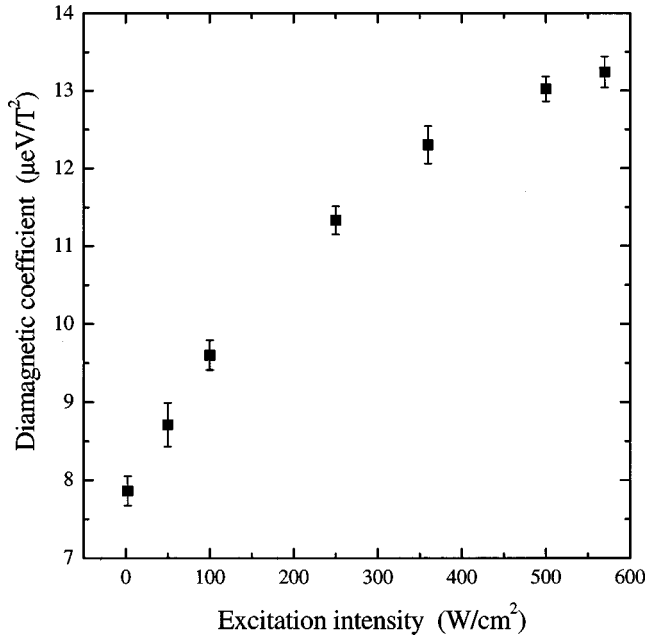


FIG. 4. Measured diamagnetic coefficient of the QD ground-state emission as a function of the excitation intensity.

where $\langle \rho^2 \rangle$ is the mean square of the in-plane electron-hole separation, $\langle \rho^2 \rangle = \langle \rho_{eh}^2 \rangle$, in the weak-confinement limit, or the mean-square of the extent of the single-particle wave functions assuming equal values for the electrons and holes, $\langle \rho^2 \rangle = \langle \rho_e^2 \rangle = \langle \rho_h^2 \rangle$, in the strong-confinement limit. In the general case, there is a competition between the lateral confinement and the Coulomb interaction. The expectation value $\langle \rho^2 \rangle$ can be expressed by³³

$$\langle \rho^2 \rangle = \lambda \langle \rho_{eh}^2 \rangle + (1 - \lambda)^2 \langle \rho_e^2 \rangle, \quad (2)$$

where the parameter

$$\lambda = 1 - \frac{\langle \rho_{eh}^2 \rangle}{2 \langle \rho_e^2 \rangle} \quad (3)$$

serves to characterize the relative strength of the lateral confinement and the Coulomb interaction. The values of $\sqrt{\langle \rho^2 \rangle}$ determined from the measured diamagnetic coefficients and the reduced mass of $\mu = 0.053m_0$ are given in Table I.

The ground-state single-particle wave function in dots with a parabolic lateral potential is given by^{20,34}

$$\Psi_i(\mathbf{r}) = \frac{1}{\sqrt{\pi} l_i} \exp\left(-\frac{r^2}{2l_i^2}\right) g_i(z), \quad i = e, h \quad (4)$$

where $g_i(z)$ is the electron (hole) wave function in the z direction, $l_i = \sqrt{\hbar^2/E_i m_i}$ is the effective length, and E_i is the electron (hole) lateral confinement energy. Then, the expectation values $\langle \rho_e^2 \rangle$ and $\langle \rho_h^2 \rangle$ for uncorrelated particles are simply given by the square of the effective lengths. Taking

into account that for the QD's studied here $E_h/E_e = 1/1.85$ (Ref. 35) and using the carrier effective masses determined above ($m_e = 0.081m_0$ and $m_{hh} = 0.153m_0$), we find that $l_e \approx l_h = 5.67$ nm. This value matches very well the value of $\sqrt{\langle \rho^2 \rangle}$ at an excitation intensity $I_{exc} = 570$ W/cm², implying that the diamagnetic shift at the highest excitation is almost entirely a result of the lateral confinement, i.e., $\lambda \approx 0$. Since the extent of the single-particle wave function is intensity independent, the smaller values of $\sqrt{\langle \rho^2 \rangle}$ at lower excitation intensities suggest a smaller electron-hole separation, i.e., a strong Coulomb interaction. In spite of the simplicity of this analysis, it obviously indicates that the increase of the diamagnetic shift with the excitation intensity should be attributed to a reduced Coulomb interaction due to the screening. Note that although the screening effect has been suggested to significantly influence the PL spectra of highly excited QD's,^{10,14,36} the observed intensity dependence of the diamagnetic shift reported here is an experimental confirmation of this fact.

Finally, we focus on the magnetic field dependence of the WL emission. As can be expected, the peak exhibits a larger shift than the QD's ground-state emission due to the smaller confinement in the WL (Fig. 3). The shift is quadratic with the field up to about 8 T and linear at higher fields. The quadratic part of the field dependence yields a diamagnetic coefficient of $\gamma_2 = 3.64 \times 10^{-5}$ eV/T². Assuming a purely 2D excitonic character of the WL emission, i.e., $\langle \rho^2 \rangle = 3/8 a_B^2$, where a_B is the 3D exciton Bohr radius, we obtain a reduced mass of $\mu = 0.052m_0$, almost the same as that of the QD's.

V. CONCLUSIONS

We have studied the magnetoluminescence spectra of InAs/GaAs self-assembled quantum dots. Using different excitation intensities, the dots are filled with up to 11–12 electron-hole pairs and the excited-state emissions are observed. The results demonstrate that the magnetic field evolution of the emission peaks can be adequately described by a single-particle model for QD's with an axial symmetry. From the measured splitting of the excited-state emission, which is found to be intensity independent, a reduced electron-hole mass much larger than the bulk InAs has been deduced. To interpret this high value, a calculation of the electron and heavy-hole effective masses has been performed within the $\mathbf{k} \cdot \mathbf{p}$ model, taking into account the effects of strain and band nonparabolicity. We also report on the diamagnetic shift of the ground-state emission of QD's and estimate the extent of the wave function at different excitation intensities. The intensity dependence of the diamagnetic shift has been analyzed in view of the relative contribution of the lateral confinement and the Coulomb interaction. The increase of the diamagnetic coefficient with the excitation intensity is attributed to the increase of the in-plane electron-hole separation, implying a screening of the Coulomb interaction in highly excited QD's.

*Electronic address: plapa@ifm.liu.se

¹See, for example, D. Bimberg, M. Grundmann, and N. Ledentsov, *Quantum Dot Heterostructures* (Wiley, Chichester, 1998).

²B. Adolph, S. Glutsch, and F. Bechstedt, *Phys. Rev. B* **48**,

15 077 (1993).

³D. Leonard, K. Pond, and P. M. Petroff, *Phys. Rev. B* **50**, 11 687 (1994).

⁴J. Y. Marzin, J. M. Gérard, A. Israel, D. Barrier, and G. Bastard,

- Phys. Rev. Lett. **73**, 716 (1994).
- ⁵M. Grundmann, N. N. Ledentsov, R. Heitz, L. Eecky, J. Christen, J. Böhrer, D. Bimberg, S. S. Ruvimov, P. Werner, U. Richter, J. Heidenreich, V. M. Ustinov, A. Yu. Egorov, A. E. Zhukov, P. S. Kop'ev, and Zh. I. Alferov, Phys. Rev. Lett. **74**, 4043 (1995).
- ⁶A. Wojs, P. Hawrylak, S. Fafard, and L. Jacak, Physica E **2**, 603 (1998).
- ⁷P. D. Wang, J. L. Merz, S. Fafard, R. Leon, G. Medeiros-Ribeiro, M. Oestreich, P. M. Petroff, K. Uchida, N. Miura, H. Akiyama, and N. Sakaki, Phys. Rev. B **53**, 16 458 (1996).
- ⁸U. Bockelmann, W. Heller, and G. Abstreiter, Phys. Rev. B **55**, 4469 (1997).
- ⁹I. E. Itskevich, M. Henini, H. A. Carmona, L. Eaves, P. C. Main, D. K. Maude, and J. C. Portal, Appl. Phys. Lett. **70**, 505 (1997).
- ¹⁰M. Sugawara, Y. Nakata, K. Mukai, and H. Shoji, Phys. Rev. B **55**, 13 155 (1997).
- ¹¹M. Bayer, S. N. Walck, T. L. Reinecke, and A. Forchel, Phys. Rev. B **57**, 6584 (1998).
- ¹²A. Polimeni, S. T. Stoddart, M. Henini, L. Eaves, P. M. Main, K. Uchida, R. K. Hayden, and N. Miura, Physica E **2**, 662 (1998).
- ¹³A. Kuther, M. Bayer, A. Forchel, A. Gorbunov, V. B. Yimofeev, F. Schäfer, and J. P. Reithmaier, Phys. Rev. B **58**, R7508 (1998).
- ¹⁴M. Bayer, A. Schmidt, A. Forchel, F. Faller, T. L. Reinecke, P. A. Knipp, A. A. Dremin, and V. D. Kulakovskii, Phys. Rev. Lett. **74**, 3439 (1995).
- ¹⁵R. Rinaldi, P. V. Guigno, R. Cingolani, H. Lipsanen, M. Sönanen, J. Tulkki, and J. Ahopelto, Phys. Rev. Lett. **77**, 342 (1996).
- ¹⁶S. Raymond, P. Hawrylak, C. Gould, S. Fafard, A. Sachrajda, M. Potemski, A. Wojs, S. Charbonneau, D. Leonard, P. M. Petroff, and J. L. Merz, Solid State Commun. **101**, 883 (1997).
- ¹⁷L. R. Wilson, D. J. Mowbray, M. S. Skolnick, M. Morifuji, M. J. Steer, I. A. Larkin, and M. Hopkinson, Phys. Rev. B **57**, R2073 (1998).
- ¹⁸S. Nomura, L. Samuelson, M.-E. Pistol, K. Uchida, N. Miura, T. Sugano, and Y. Aoyagi, Appl. Phys. Lett. **71**, 2316 (1997).
- ¹⁹J. M. Garcia, T. Mankad, P. O. Holtz, P. J. Wellman, and P. M. Petroff, Appl. Phys. Lett. **72**, 3172 (1998).
- ²⁰A. Wojs, P. Hawrylak, S. Fafard, and L. Jacak, Phys. Rev. B **54**, 5604 (1996).
- ²¹I. E. Itskevich, M. S. Skolnick, D. J. Mowbray, I. A. Trojan, S. G. Lyapin, L. R. Wilson, M. J. Steer, M. Hopkinson, L. Eaves, and P. C. Main, Phys. Rev. B **60**, R2185 (1999).
- ²²M. Grundmann, N. N. Ledentsov, O. Siew, J. Böhrer, D. Bimberg, V. M. Ustinov, P. S. Kop'ev, and Zh. I. Alferov, Phys. Rev. B **53**, R10 509 (1996).
- ²³G. Medeiros-Ribeiro, D. Leonard, and P. M. Petroff, Appl. Phys. Lett. **66**, 1767 (1995).
- ²⁴U. Bockelmann, Phys. Rev. B **50**, 17 271 (1994).
- ²⁵V. Halonen, T. Chakraborty, and P. Pietiläinen, Phys. Rev. B **45**, 5980 (1992).
- ²⁶P. D. Wang, N. N. Ledentsov, C. M. Sotomayor Torres, I. N. Yassievich, A. Pakhomov, A. Yu. Egorov, P. S. Kop'ev, and V. M. Ustinov, Phys. Rev. B **50**, 1604 (1994).
- ²⁷M. A. Cusack, P. R. Briddon, and M. Jaros, Phys. Rev. B **56**, 4047 (1997).
- ²⁸R. People and S. K. Sptz, Phys. Rev. B **41**, 8431 (1990).
- ²⁹C. G. Van de Walle, Phys. Rev. B **39**, 1871 (1989).
- ³⁰J. Brubach, A. Yu. Silov, J. E. M. Haverkort, W. Van der Vleuten, and J. H. Wolter, Superlattices Microstruct. **21**, 527 (1997).
- ³¹K. Yoh, H. Kazama, and T. Nakano, Physica B **249–251**, 243 (1998).
- ³²M. Fricke, A. Lorke, J. P. Kotthaus, G. Medeiros-Ribeiro, and P. M. Petroff, Europhys. Lett. **36**, 197 (1996).
- ³³S. N. Walck and T. L. Reinecke, Phys. Rev. B **57**, 9088 (1998).
- ³⁴R. J. Warburton, B. T. Miller, C. D. Durr, C. Bödefeld, K. Karrai, J. P. Kotthaus, G. Medeiros-Ribeiro, P. M. Petroff, and S. Hant, Phys. Rev. B **58**, 16 221 (1998).
- ³⁵H. Schmidt, G. Medeiros-Ribeiro, M. Oestreich, P. M. Petroff, and G. H. Döhler, Phys. Rev. B **54**, 11 346 (1996).
- ³⁶R. Rinaldi, R. Mangino, R. Cingolani, H. Lipsanen, M. Sönanen, J. Tulkki, M. Brasken, and J. Ahopelto, Phys. Rev. B **57**, 9763 (1998).